

Proceedings of the Fifth International Conference on
Railway Technology:
Research, Development and Maintenance
Edited by J. Pombo
Civil-Comp Conferences, Volume 1, Paper 21.24
Civil-Comp Press, Edinburgh, United Kingdom, 2022, doi: 10.4203/ccc.1.21.24
©Civil-Comp Ltd, Edinburgh, UK, 2022

Spalling defect of head-hardened rail in railway turnouts

M. Messaadi¹, M. Steenbergen² and I. Shevtsov³

¹MSMP-EA7350, Arts et métiers ParisTech, Lille, France

**²Delft University of Technology, Section of Railway Engineering,
Faculty of Civil Engineering and Geoscience,
Delft, The Netherlands**

**³ProRail, Department of Civil Technology, Infra Management
Rail-Systems, Utrecht, The Netherlands**

Abstract

This paper investigates the spalling degradation process that could be involved in railway turnouts. By considering the network's failed rails, metallographic examinations revealed the development of subsurface micro-cracks attributed mainly to the non-metallic inclusions. Using Murakami & Yanase equations, the critical size of inclusions leading to the subsurface initiation is discussed in the case of a head-hardened rail (350HT) and a standard one (R260). Our findings suggest that the available studies, such as the Kitagawa-Takahashi diagram, overestimate this size on the rail's top surface.

Keywords: head-hardened rails, turnouts loading, rail surface defects, surface and sub-surface cracking, non-metallic inclusions, non-metallic inclusions, surface hardness profile

1 Introduction

Rolling contact fatigue (RCF) generates various degradation features on rail surfaces, for instance, squats, studs, and wear. The spalling process occurs also in rails and could lead to the loss of the train operation in severe cases. Rail spalling consists of the break of the rail top surface into small metal fragments. It appears as hollows across the running band leading to geometrical discontinuity of the wheel-rail contact patch. Depending on the size and the length of the spalled area, it could affect the train dynamics as other rolling contact fatigue defects [1]; squats, and corrugation. The basic rail spalling literature reports that the most dangerous forms are avoided in the case of head-hardened rails [2–5].

Since 1991, Dikshit et al. studied ‘deep spalling’ that appeared in the center of the running band of curved rails [2]. They inferred that the spall is associated with the early development of the tribological transformed surface (TTS) called the white etching layers (WELs). In recent years, Steenbergen examined another form of spalling described to be a ‘periodic spalling defect’ [4]. He indicated that rolling contact fatigue behavior in standard and heat-treated pearlitic rails differs; the standard grade seems to take off WELs layers during service when the heat-treated develops extensive surface cracks as grinding residual WELs may be pressed into the pearlitic matrix [6]. To toe the line with these findings, Pereira et al. detailed the role of the WELs in the initiation through rigorous metallurgical investigation of a severe spalling form [5].

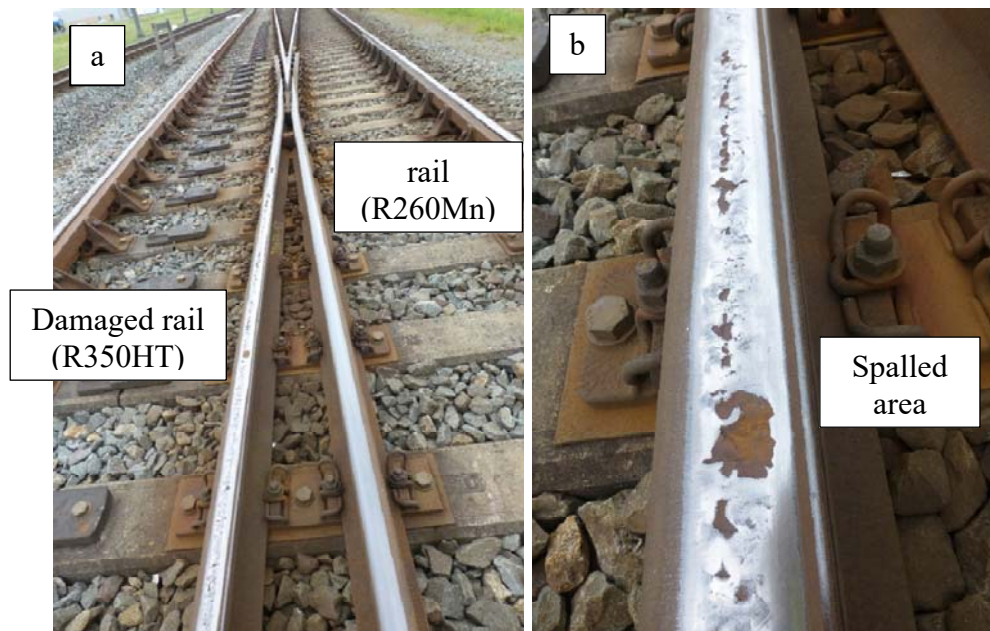


Figure 1. Switch defects observed in the Dutch network; a-overview of the switch, b- Spalling defects on the switch running rail.

This work reports also a metallographic investigation of spalling defects that occurred in the turnouts area where it is often reported and rarely characterized. There

is almost no published literature on this subject. Additionally, the field inspections showed that the damage was spread into the head-hardened grade rather than the standard. Figure 1-a presents an overview of an investigated switch. It confirms the difference in damage processes in rail grades. In the same track location, the head-hardened rail exhibits a harmful running band compared to the neighbor rail made from a standard grade. Figure 1-b details the spalling aspects. It shows various and discontinuous spalled areas coexisting with an extensively deformed surface.

That is why this paper attempts to explain the dissimilar spall processes. With regards to the specific loading history of switches and crossings (S&C); high loading (impacts) and vibrational environment (variability of the track support stiffness) [7], the evident interrogation is whether and how the WELs contribute to spalling defect development. Is it a comparable scenario to the curved lines wearing processes?

The paper is divided into three sections in addition to the introduction. The second section presents an inspection of the various spalling forms in S&C rails. Moreover, it indicates the characterization methodology. The third section displays the metallographic cross-sectioning results pointing out the subsurface cracking. Besides, it discusses and explains the vulnerability of head-hardened grades. The paper ends with conclusions as to the fourth and last section.

2 Methods

2.1. Rails collected from the track

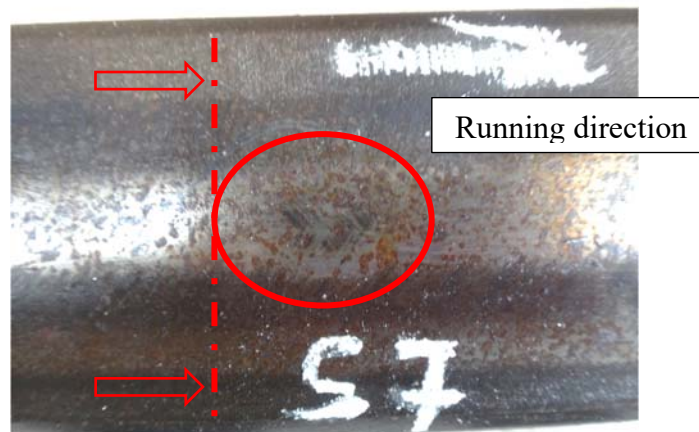


Figure 2. The appearance of the early-stage defect.

Defective turnout rails are collected from the Dutch network; the Betuweroute location. It is known to be a heavily laden track. In general, the research plan focuses on the defect's assessment consisting of a metallographic investigation at different levels of spall severity across the running rail (see Figure 1. b). Collected rails are head-hardened grade R350HT.

This paper presents the results of exclusively one damage type named an ‘early-stage spalling defect’. Figure 2 presents his appearance where the only groovy surface is marked in the middle of the running band. Obviously, it is a distinct feature compared to rolling contact fatigue failing forms described elsewhere [8]. This suggests also that the defect development scenario may differ.

2.2. Metallographic investigations

It consists of laboratory investigations using TU Delft facilities (3mE faculty). The defected area is carefully sectioned from the rail head along the transversal direction; a cutting illustration is provided in Figure 2. After that, the specimen was cold-mounted and manually polished up to 3 μ m diamond solution. Succession between mirror polishing and optical microscopy observations was adapted in order to meticulously inspect the cross-section specifically the presence of surface or subsurface cracks. It was also important to etch the sample to check the presence of the white etching layers mainly the running band region.

The microstructure examinations were carried out using the digital Keyence microscope VHX-5000 offering a multi-scale investigation. For finer analysis, investigations were performed using the scanning electron microscope JEOL JSM 7500F (SEM) coupled within EDS.

2.3. The head-hardened grade R350HT

Head-hardened grades have pearlite microstructure as the standard ones. The strengthening of these steels occurs either by alloying and/or heat treatment. For the 350HT grade, the chemical composition is comparable to the R260 one which undergoes a specific heat treatment (HT). This induces a finer microstructure enhancing the rail-head hardness from 260 to 350 HB. Further details concerning their microstructures and mechanical properties are available elsewhere [9] [10].

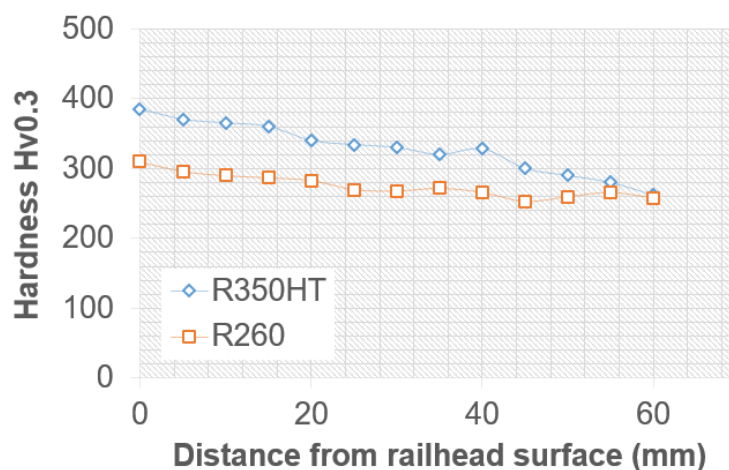


Figure 3. Hardness profile measured in the transversal direction of rail heads: R260 standard grade and the R350HT from [10].

Figure 3 illustrates the hardness profiles along the railhead of the two grades. Obviously, the head-hardened grade has a higher hardness that is decreasing until reaching a comparable value to the standard grade. This difference in hardness distribution affects the ratcheting and the damaging behavior of steels. The author thinks that still a crucial point not well discussed in the literature concerning the clearness of these grades. In another word, the amount of non-metallic inclusions, oxides, and voids present in the microstructure.

It can be assumed that similar quantities and morphologies of these inhomogeneities exist and affect fatigue strength differently (as two steel have almost the same chemical composition). Regarding literature, the correlation between the steel hardness and the fatigue strength in an inclusion neighbour is proposed by Murakami et al [11]. This study explores the case of internal inclusion which means the void/ inclusion is located in the subsurface according to the following equation:

$$\sigma_e = \frac{1.56 \cdot (HV + 120)}{(\sqrt{area})^{1/6}} \left[\frac{1 - R}{2} \right]^\alpha \quad (1)$$

With σ_e is the fatigue endurance limit (amplitude) of the material at $R=-1$ (see table 1), HV Vickers hardness, \sqrt{area} , the square root of the defect area normal to the loading direction, $\alpha = 0.226 + HV \cdot 10^{-4}$.

3 Results

3.1. Metallographic expertise

The metallographic expertise of the spalling defect revealed the presence of subsurface cracks. Figure 4-a presents an overview of the transversal cross-section showing the wings crack type. It shows bidirectional cracks initiated from subsurface voids at around 1 mm underneath the surface. In the gauge corner side, cracks grow into the material generating successive cracks clusters (see Figure 4-b). Meanwhile, on the field corner side, the subsurface cracks seem to be unconnected and appear parallel with different lengths as illustrated in Figure 4-c.

Regarding the literature, a comparable crack feature was reported by Grassiel et al. in the case of stud defect however no clusters were reported [12]. Besides, a crucial difference in comparison to the stud defect is the absence of the white etching layers and the plastic deformation above the wings crack. The metallographic investigation shows no white etching layer and no accumulated plastic flow in Figure 4-d.

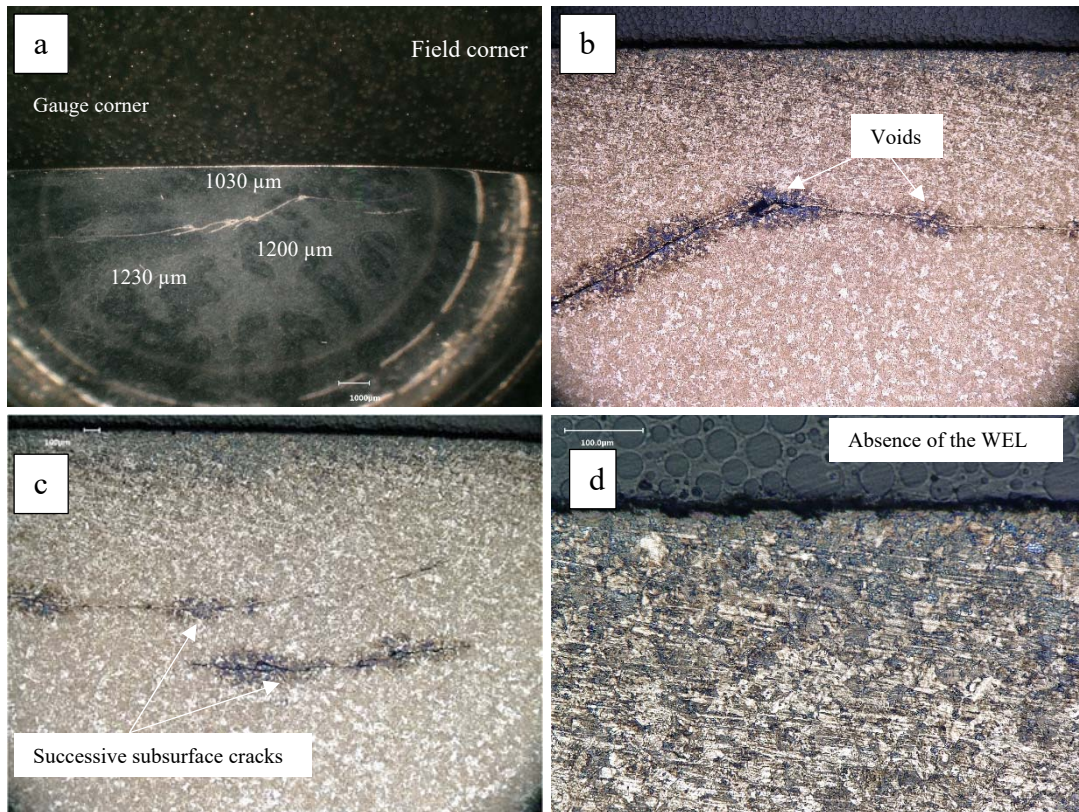


Figure 4. Optical microscopy observations of the early-stage defect cross-section.

It is important to check the presence of these layers as the RCF surface cracks are usually attributed to their spread. In fact, the metallurgical heterogeneity within the steel matrix and its weakness lead to an acceleration of rail surface cracking. Nevertheless, our metallurgical investigation suggests that the incubation time to become a visible spall defect is governed by subsurface cracking and propagation.

Figure 5 depicts two illustrative images; figure 5-a presents an example of a cracks cluster showing the clear repetitive bifurcation of cracks front. Further, it shows also that small pieces of the steel matrix could be delaminated inside the material. The second image, figure 5-b, indicates that cracks are active as they could delaminate the crack edges leading to close some cracks patterns.

Additional information can draw from figure 5-a about the non-metallic inclusions that seem to be present along the crack path. This is also reported in several rail research works [13] [14]. The missing link to understanding the exclusive spread of the spalling defect could be the overcharging of the inclusion neighbor in the head-hardened rail rather than the standard one. This is would be further considered in the following section.

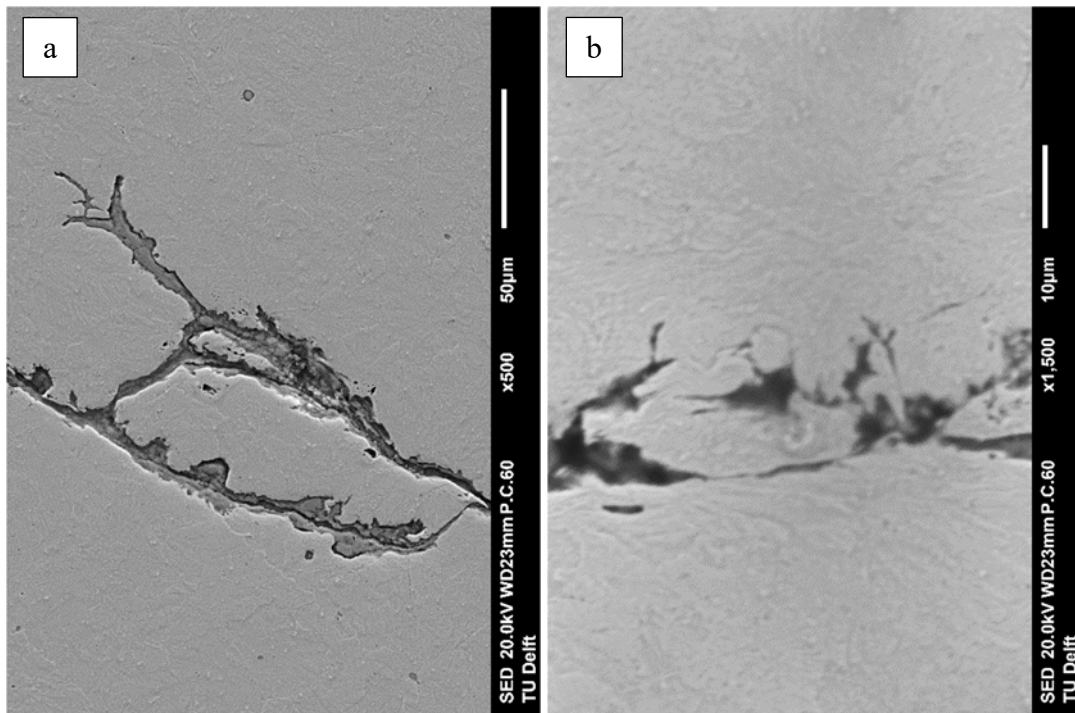


Figure 5. Scanning electron microscopy observations of subsurface cracks of figures 4-a and c. a- Example of a crack cluster, b-Plastic deformation of the crack pattern edges.

3.2. Discussion

The critical inclusion size is evaluated by the fatigue design criteriums such as El-Haddad mode [15] and the Carpinteri et al. criterion [16] ... For switches components, Kolitsch et al. investigated this relationship for both the manufacturing processes and also for loads generated by train passage [17]. Their approach is based on the estimation of the bending stresses (and strain) in combination with the concept of linear elastic fracture mechanics (LEFM) and elastic-plastic fracture mechanics (EPFM). Various rail grades are compared. The Kitagawa-Takahashi diagram in [17] summarizes these findings. Nevertheless, this approach is missing to consider the wheel-rail contact loading.

More recently, Kato et al. investigated the correlation between the rolling contact stresses and the subsurface inclusion critical size for wheels [15]. Using the model developed by El-Haddad, they proposed diagrams relating the shear fatigue stress (experimentally simulated by torsion load) and the axial fatigue to the defect size. To toe the lien with the rolling contact loading, they performed a numerical simulation to access the shear stress in the subsurface.

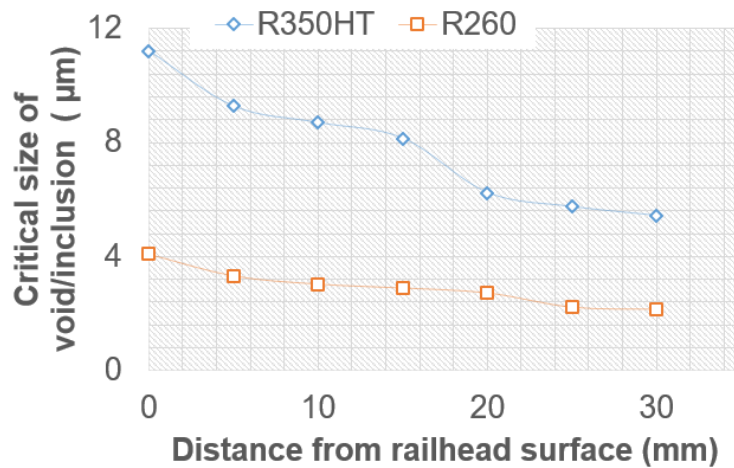


Figure 6. Comparison of subsurface cracking susceptibility between R260 and R350HT for an endurance shear limit of 350MPa.

Assuming that rail steels have comparable shear fatigue endurance of $\sigma_e = 350\text{MPa}$, figure 6 compares the evolution of inclusion size leading to crack initiation along the transversal profile of the rail head based on hardness reported in figure 3. It shows clearly that the R350HT is more susceptible to subsurface cracks. It is important to indicate that these results overestimate the critical size as no calculation has been performed to evaluate the sub-surface shear stress. Meanwhile, the 350MPa is a realistic stress value achievable in rail loading [17]. Considering these results, future work would focus further on the study of the estimation of fatigue limits and the cracking mechanism in the early stage of rail.

4 Conclusions and Contributions

This study deals with the characterization of spalling defect spread into a head-hardened rail. It puts forward a metallographic examination and estimates the critical size of the subsurface inclusion based on Murakami and Yanase criteria. Conclusions drawn from this research are the following:

- Subsurface cracks are omnipresent in all stages of spalling defect development.
- The investigation of an early-stage defect showed long and bifurcated cracks in the subsurface.
- No WELs were observed in the case of early-stage defects.

The vulnerability of the head-hardened rail seems to be attributed to the decrease in its hardness causing a low fatigue limit around the small size of inclusions compared to the standard grades.

Acknowledgments

The authors would like to thank the Dutch Rail Infrastructure owner ProRail, and ID2 for their support: Ruud Van Bezooijen for the field-testing arrangement and the track facilities.

References

- [1] C. Liu, J. Xu, K. Wang, T. Liao, P. Wang, Numerical investigation on wheel-rail impact contact solutions excited by rail spalling failure, *Eng. Fail. Anal.* 135 (2022) 106116.
- [2] V. Dikshit, P. Clayton, D. Christensen, Investigation of rolling contact fatigue in a head-hardened rail, *Wear.* 144 (1991) 89–102.
- [3] A.C. Athukorala, D. V. De Pellegrin, K.I. Kourousis, A unified material model to predict ratcheting response in head-hardened rail steel due to non-uniform hardness distributions, *Tribol. Int.* 111 (2017) 26–38.
- [4] M. Steenbergen, Rolling Contact Fatigue: spalling versus transverse fracture of rails, *Wear.* 380–381 (2017) 96–105.
- [5] J.I. Pereira, G. Tressia, E.J. Kina, A. Sinatora, R.M. Souza, Analysis of subsurface layer formation on a pearlitic rail under heavy haul conditions: Spalling characterization, *Eng. Fail. Anal.* 130 (2021) 105549.
- [6] M. Steenbergen, Rolling contact fatigue in relation to rail grinding, *Wear.* 356–357 (2016) 110–121.
- [7] I. Grossoni, P. Hughes, Y. Bezin, A. Bevan, J. Jaiswal, Observed failures at railway turnouts: Failure analysis, possible causes and links to current and future research, *Eng. Fail. Anal.* 119 (2021) 104987.
- [8] S L Grassie, D I Fletcher, E A Gallardo Hernandez, and P Summers, Studs: a squat-type defect in rails, *Proc. IMechE Vol. 226 Part F: J. Rail and Rapid Transit* (2011).
- [9] Ali motameni tabatabaei, Fracture and fatigue crack growth characterization of conventional and head hardened railway rail steels, thesis, The Graduate School of Natural and Applied Sciences of Middle East Technical University, 2014.
- [10] P.Christoforou, D.I. Fletcher, R.Lewis, Benchmarking of premium rail material wear, *Wear*, Volumes 436–437, 15 October 2019, 202990.
- [11] Y. Murakami, S. Kodama and S. Konuma, Quantitative evaluation of effects of non-metallic inclusions on fatigue strength of high strength steels. I : Basic fatigue mechanism and evaluation of correlation between the fatigue fracture stress and the size and location of non-metallic inclusions, *Int J Fatigue* 11 No 5 (1989) pp 291-298.
- [12] Stuart L Grassie, David I Fletcher, Ezequiel Alberto Gallardo Hernandez, Paul Summers, ‘Studs’: A squat-type defect in rails, *Proceedings of the Institution of Mechanical Engineers, Part F: Journal of Rail and Rapid Transit* , 226 (3). pp. 243-256. ISSN 0954-4097.
- [13] K. V. Grigorovich, A. S. Trushnikova, A. M. Arsenkin, S. S. Shibaev, and A. K. Garber, Structure and Metallurgical Quality of Rail Steels Produced by

- Various Manufacturers, ISSN 0036-0295, Russian Metallurgy (Metally), Vol. 2006, No. 5, pp. 427–438. © Pleiades Publishing, Inc., 2006.
- [14] J.E. Garnham, R.-G. Ding, C.L. Davis, Ductile inclusions in rail, subject to compressive rolling–sliding contact, *Wear* 269 (2010) 733–746.
- [15] T. Kato , T. Fujimura, Y. Yamamoto, S. Dedmon, S. Hiramatsu, H. Kato, Y. Kimura, J. Pilch, Critical internal defect size for subsurface crack initiation in heavy haul car wheels, *Wear* 438-439 (2019) 203038.
- [16] Sabrina Vantadori , Camilla Ronchei , Daniela Scorza , Andrea Zanichelli , Lucas Carneiro Araújo, Jos´e Alexander Araújo, Influence of non-metallic inclusions on the high cycle fatigue strength of steels, *International Journal of Fatigue* 154 (2022) 106553.
- [17] Stefan Kolitscha, Hans-Peter Gänser, Reinhard Pippan, Damage Tolerance Concepts for Railway Switch Components, ESIS TC24 Workshop "Integrity of Railway Structures", 24-25 October 2016, Leoben, Austria, *Structural Integrity Procedia* 00 (2016) 000–0.